RSC Advances

PAPER

View Article Online
View Journal | View Issue

Cite this: *RSC Adv.*, 2017, **7**, 28841

Non-isocyanate polyurethane/epoxy hybrid materials with different and controlled architectures prepared from a CO_2-sourced monomer and epoxy *via* an environmentally-friendly route†

Jiexi Ke,[ab] Xiaoyun Li,[ab] Feng Wang,[a] Shuai Jiang,[ab] Maoqing Kang,[a] Junwei Wang,[*ac] Qifeng Li[a] and Zhijie Wang[c]

Polyurethane/epoxy hybrid materials from CO_2-sourced monomer were prepared *via* an environmentally-friendly and non-toxic route, which avioded the use of toxic isocyanate. A series of non-isocyanate polyurethane (NIPU)/epoxy hybrid materials, with different and controlled architectures, were synthesized from CO_2, polypropylene glycol diglycidyl ether (PPGDGE), amines and diglycidyl ether of bisphenol-A (BADGE). Around 12 wt% CO_2 was incorporated into PPGDGE to form a five-membered cyclic carbonate (5CC-PPGDGE). The complete conversion and selectivity of PPGDGE were obtained. The kinetics of 5CC-PPGDGE was investigated by reacting it with 1,2-ethylenediamine (EDA) at different temperatures. NH_2-terminated pre-polymers were obtained by reacting 5CC-PPGDGE with various excessive amines. Finally, the hybrid materials were obtained by curing pre-polymers with BADGE. The results showed that a high content of amine with more functional groups led to better mechanical performances than diamine-based hybrid materials. This is the first time that architectures have been controlled by altering the amine ratio and functionality. And these hybrid materials exhibited satisfactory mechanical performances. The DETA-based and TETA-based materials with high amine ratio exhibited a tensile strength of 15.0 MPa and 12.5 MPa, accompanied with elongation at break of 151.3% and 170.9%, respectively. The gel content, glass transition temperature and thermodynamic stability went up first and then declined with the increase of amine ratio, which demonstrated the architectures of hybrid materials ranged from defective to cross-linked and linear structures.

Received 13th April 2017
Accepted 24th May 2017

DOI: 10.1039/c7ra04215a

rsc.li/rsc-advances

1. Introduction

Over the past several decades, the atmospheric level of CO_2 concentration has been increasing at a rapid rate as a result of the consumption of chemical resources *via* means such as industrial emission and vehicle emission.[1] CO_2 is one of the most significant greenhouse gases which cause global warming and climate change. Meanwhile, CO_2 is also an easily available, recyclable, abundant, nontoxic as well as inexpensive resource.[2] The conversion and transformation of it into valuable chemicals and materials is an important subject from the viewpoint of environmental protection and resource utilization.[3,4] One of the most attractive reactions for CO_2 utilization is the synthesis of five-membered cyclic carbonates (5CC) with epoxide substrates. The cyclic carbonate can be used for various purposes, such as aprotic polar solvents, fuel additives, electrolytes and intermediates for polymer synthesis.[5,6] And many researchers have devoted effort to the synthesis of cyclic carbonates, such as Chen *et al.*[7]

In recent years, the utilization of 5CC acting as CO_2-sourced monomer to produce polyurethane (the so-called non-isocyanate polyurethane (NIPU)) has attracted considerable attention due to avoiding the use of toxic feedstock during the preparation process. It is well known that the traditional polyurethane (PU) is usually synthesized from toxic isocyanate and polyol.[8–10] However, during preparation process of PU, the repetitive exposure to isocyanate can lead to serious and incurable harm to human health.[11] Besides, the synthesis of isocyanates, for methane dipheyl 4,4′-diisocyante as example, requires toxic phosgene.[12]

Thus, the preparation of NIPU originating from aminolysis reaction of 5CC with amine can be effective for CO_2 utilization and avoid the use of noxious isocyanates.[13] Very recent

[a]*Institute of Coal Chemistry, Chinese Academy of Sciences, Taiyuan 030001, China*
[b]*University of Chinese Academy of Sciences, Beijing 100049, China*
[c]*National Engineering Research Center for Coal-Based Synthesis, Changzhi, 030001, China. E-mail: wangjw@sxicc.ac.cn*

† Electronic Supplementary Information (ESI) available. See DOI: 10.1039/c7ra04215a

reviews[14–18] reported comprehensive studies and summarized the reaction between 5CC and amines. It fits in with the viewpoint of "green chemistry" quite well. Compared with the traditional PU containing urethane group in main chain, NIPU also has hydroxyl groups throughout the molecular chain. The hydrogen atom of hydroxyl promotes intermolecular hydrogen formation with the carbonyl oxygen atom of urethane group.[19] This formation improves the hydrolytic and thermodynamic stability for the NIPU materials. Various chemicals with different structures are used as reactants to prepare NIPU. The cyclic carbonate and amine with aliphatic, cycloaliphatic or aromatic structures are studied, which are similar to the traditional isocyanates.[20] The polypropylene glycol diglycidyl ether (PPGDGE),[21,22] diglycidyl ether of bisphenol A (BADGE),[23] and renewable plant oil[24,25] are the main monomers or oligomers for cyclic carbonate synthesis. For instance, polypropylene glycol diglycidyl ether (PPGDGE) can be obtained from renewable glycerol which is a by-product during the preparation process of biodiesel.[26–28] However, due to side reaction and low reactivity between 5CC and amine,[29] it is difficult to obtain high molar masses and form the cross-linkage among the main chain as traditional PU. The formation of urea, oxazolidinone and dehydration products is seriously suspected to be responsible for the low molar masses during the NIPU syntheses. In addition, the steric hindrance and ring strain of cyclic carbonate take part of responsibility for low molar mass and poor cross-linkage.[30] Therefore, to resolve these problems, many groups focus on the improvement of NIPU by studying the relationship between performance and structure, *e.g.* Figovsky and co-workers[31] reported the synthesis of hybrid NIPU materials from carbonated soybean oil and bisphenol resin *via* a two-step pathway. In addition, several groups have reported the preparation of analogous NIPU elastomer which is derived from the modified amine.[32–34] Although the several methods are taken to improve the properties of NIPU, the performances of it are unsatisfactory for practical application.

In this study, a new method is developed to enhance the performances of NIPU. As our previous report,[35] BADGE could be introduced to NIPU materials to improve the cure rate and increase cross-linkage. The non-toxic polyurethane materials were obtained *via* an environment-friendly route, in substituting toxic isocyanate by 5CC, amines with different functional groups as well as BADGE. The 5CC as a CO_2-monomer was synthesized by a cyclo-addition reaction from bio-based PPGDGE and CO_2, which was low-cost and abundant. And the kinetics of it was studied. Then, series of NH_2-terminated pre-polymers with different molecular mass and structure were obtained by ring-opening reaction of 5CC with excessive diamine and polyamines. Finally, the BADGE could act as chain extender to cure the soft pre-polymers and to provide cross-linkage for hybrid materials. Most importantly, this is the first time to control the architectures of NIPU/epoxy hybrid materials by varying the ratio of amine to 5CC (abbreviated as amine ratio hereafter) and amine functionality. The properties of these NIPU/epoxy hybrid materials with controlled architecture were studied by Fourier Transform Infrared Spectra (FTIR), scanning electron microscopy (SEM), X-ray diffraction (XRD), swelling analysis, tensile performance, *etc.*

2. Experimental

2.1 Materials

The polypropylene glycol diglycidyl ether (PPGDGE) (number-average molecular mass = 650 g mol^{-1}) and poly(-glycoldiglycidyl) ether (PEGDGE) were purchased from Wuhan Yuanchen technology Co., China. Propylene carbonate was supplied by Sinopharm Chemical Reagent Co., Ltd. The quaternary ammonium salt modified amberlyst (D296) was purchased from Tianjin Resin Technology Co., China. The epoxy resin based on diglycidyl ethe of bisphenol A (BADGE) with epoxy oxygen content (EOC) of 0.534 g mol^{-1} was purchased from Zhejiang Bangfeng Plastic Co., China. 1,2-Ethylenediamine (EDA), diethylenetriamine (DETA), triethylenetetramine (TETA), and triethylenediamine (TEDA) were obtained from Sinopharm Chemical Reagent Beijing Co., Ltd. CO_2 (99.99%) was commercially available and kindly supplied by Shanxi Institute of Coal Chemistry, Chinese Academy of Sciences. All the raw materials were used as received without further purification.

2.2 Synthesis

2.2.1 Reaction of PPGDGE with CO_2. The five-membered cyclic carbonate (5CC), CO_2-sourced monomer, was prepared according to the following process (as Scheme 1). PPGDGE (100 g) and catalyst (10 wt% compared to the PPGDGE) were charged into a 500 mL autoclave. After leak test and purifying with CO_2 for 5 min, the reaction mixture was stirred and heated to 130 °C. Then, the reaction was carried out at 1 MPa CO_2 pressure for 30 h. Structural analysis of PPGDGE and CO_2-sourced product was carried out by Fourier Transform Infrared Spectra (FTIR), Nuclear Magnetic Resonance (^{1}H NMR) and elemental analysis. The cyclic carbonate equivalent weight (CEW) was measured by ^{1}H NMR. Meanwhile, reactivity of product was investigated by reacting with EDA in bulk at different temperature. The CO_2-fixed product, 5CC from PPGDGE, was abbreviated as 5CC-PPGDGE hereafter.

2.2.2 Synthesis of NH_2-terminated NIPU pre-polymer. The progress of ring-opening reaction of 5CC-PPGDGE with amine had shown in Scheme 2. 5CC-PPGDGE (60 g, 82 mmol) and amine (according to the formula) were mixed at 90 °C for 4 h with TEDA (0.3 g, 5 mmol) as catalyst. The functional groups of amine for 5CC-PPGDGE and BADGE were summarized in Table 1. For obtaining NH_2-terminated pre-polymer, the

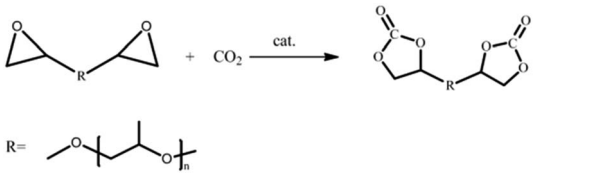

Scheme 1 The scheme of synthesis of 5CC.

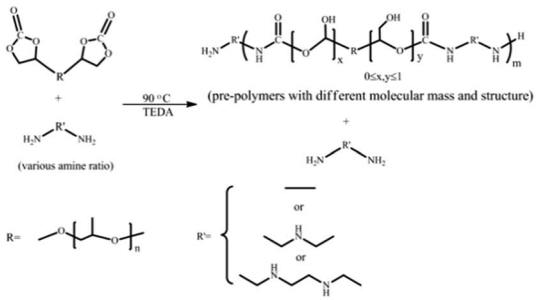

Scheme 2 The scheme of synthesis of NH_2-terminated NIPU pre-polymer.

Table 1 Information of the various types of amines

Amine type	Molecular mass (g mol^{-1})	Amine content (mmol g^{-1})	Functional groups for 5CC	Functional groups for BADGE
EDA	60	16.67	2	4
DETA	103	9.71	2	5
TETA	146	6.85	2	6

excessive amine, compared to 5CC-PPGDGE, was necessary. The detailed information was shown in Table 3. The amount of amine was calculated according to following eqn (1). For example, the EDA-based NIPU pre-polymers with different formulations were prepared with molar ratio of amine to 5CC-PPGDGE and BADGE at 0.7, 0.9, 1.1 and 1.3. Hence, the corresponding molar ratio of amine to 5CC-PPGDGE is 1.14, 1.46, 1.79 and 2.11, respectively. The pre-polymers from EDA were noted as Pre-polymer-EDA-1–Pre-polymer-EDA-4, respectively. The DETA-based and TETA-based pre-polymers were prepared with the similar formulations, which were noted as Pre-polymer-DETA-1–Pre-polymer-DETA-4 and Pre-polymer-TETA-1–Pre-polymer-TETA-4, respectively. The conversion of 5CC-PPGDGE into NIPU was calculated by eqn (2). The structure and molecular mass analysis was conducted by ^{1}H Nuclear Magnetic Resonance (^{1}H NMR), Fourier Transform Infrared Spectra (FTIR), and Gel Permeation Chromatography (GPC).

The amount of amine was calculated according to following eqn (1), of which CEW_{5CC} and m_{5CC} represented CEW and mass of 5CC-PPGDGE, EOC_{BADGE} and m_{BADGE} represented the EOC and mass of BADGE, and n represented the functional groups of amine for 5CC or BADGE.

$$n_{\text{organic amine}} = \frac{CEW_{5CC} \times m_{5CC}}{n_{\text{number of functional groups for 5CC}}} + \frac{EOC_{BADGE} \times m_{BADGE}}{n_{\text{number of functional groups for BADGE}}} \quad (1)$$

The residual cyclic carbonate ratio was determined through following eqn (2), of which I_a, I_b and I_c were integration of peak a, b and c of 5CC-PPGDGE, respectively. I'_a, I'_b, and I'_c were integration of peaks of cyclic carbonate in pre-polymer. $m_{5CC\text{-}PPGDGE}$ and $m_{\text{per-polymer}}$ were the mass of tested 5CC-PPGDGE and per-polymer, respectively.

$$\alpha\ (\%) = \frac{\dfrac{(I_a + I_b + I_c)}{m_{\text{per-polymer}}}}{\dfrac{(I'_a + I'_b + I'_c)}{m_{5CC\text{-}PPGDGE}}} \times 100 \quad (2)$$

2.2.3 Curing reaction of NH_2-terminated NIPU pre-polymer with BADGE. The NH_2-terminated NIPU per-polymers were cured by introducing BADGE to prepare final NIPU/epoxy hybrid materials. BADGE was introduced to promote the chain extending reaction and enhance the cross-linkage of those NIPU/epoxy hybrid materials. In order to eliminate bubble, the curing reaction was carried out in a vulcanizer with the condition of 8 MPa and 110 °C for one hour. Then, the post curing was conducted at 90 °C for 24 h. Due to amine ratio and amine type causing the different characteristics of pre-polymers, the final hybrid materials with various architectures were obtained (see Scheme 3). The BADGE content in final hybrid material was designed as 40 wt%. The structure and properties of NIPU/epoxy hybrid materials were performed by means of FTIR, scanning electron microscopy (SEM), X-ray diffraction (XRD), swelling in THF, mechanical tests, *etc.*

The final NIPU/epoxy hybrid materials were noted as NIPU-EDA-1–NIPU-EDA-4, NIPU-DETA-1–NIPU-DETA-4, and NIPU-TETA-1–NIPU-TETA-4 according to the corresponding pre-polymers.

2.3 Characterization methods

2.3.1 FTIR. The FTIR measurements were performed on a NICOLET-380 Fourier transform infrared instrument by using the attenuated total reflectance (ATR) of 32 scans at a resolution of 4 cm^{-1} (Thermo Electron Co., Ltd, USA).

2.3.2 ^{1}H NMR. ^{1}H NMR measurements were recorded on a Bruker Avance 400 MHz spectrometer (Bruker Co., Ltd., Switzerland) in DMSO or $CDCl_3$. The chemical shifts were reported in parts per million relative to tetramethylsilane (TMS).

2.3.3 Elemental analysis. The elemental analysis was performed on a Vario EL cube elemental analyzer (Elementar), the elemental analysis was performed on a Vario EL cube elemental

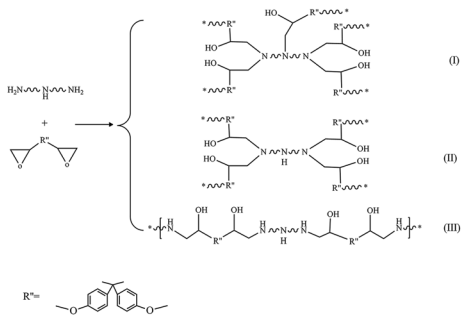

Scheme 3 Chain extension by introducing BADGE into NIPU/epoxy hybrid material.

analyzer (Elementar, Germany). The C, H, N, S test mode was adopted to analyze C, H and O of products.

2.3.4 GPC. The GPC measurements were acquired by employing Agilent 1100 chromatographic system (Agilent Co., Ltd., USA) with a Gel PW column of Nanofilm GPC-150 (Sepax Technologies Co., Ltd., USA). The measurements were carried 35 °C with a 1 mL min^{-1} flow rate of THF, calibrated using standard polystyrene. In order to obtain accurate molecular mass of NH_2-terminated pre-polymers, the excessive amine was removed for the test samples by distillation under vacuum.

2.3.5 SEM. SEM (2800B, KYKY, China) was operated at 25 kV to characterize the surface morphology of fracture surface of NIPU/epoxy hybrid materials.

2.3.6 XRD. A Bruke D8 Advance instrument (Bruker, Ettlingen, Germany) was used. The tube voltage was maintained at 40 kV and the ytube current at 100 mA. Diffraction patterns were collected at a scanning rate of 2 min^{-1} and a step size of 0.02°. A scanning of 2θ angles between 10° and 70° was carried out.

2.3.7 DMA. The dynamic thermal-mechanical properties of samples were measured by a DMA-Q800 (TA Instruments, New castle, USA) at a heating rate of 5 °C min^{-1} over a temperature range from −30 °C to 90 °C. The rectangular dimensions of the samples were 20 mm × 6 mm × 2 mm. The measurements were conducted in tensile mode with frequency of 1 Hz and amplitude of 20 μm, respectively.

2.3.8 Tensile test. Tensile properties were performed by using dumbbell-shaped specimens. Experiments were carried out at room temperature by using a CMT6503 instrument (Shenzhen Sans Testing Machine Co., Ltd., Shenzhen, China). The cross-head speed was 500 mm min^{-1}. For each formulation, at least five samples were tested to assess Young's modulus, stress at break, and elongation at break.

2.3.9 Hardness test. The hardness tests were measured using a shore rubber durometer (Jiangdu Co., Ltd, China) according to standard ASTM D1415 7619-1 specifications with a shape of 20 mm diameter and 6 mm thickness. For each formulation, at least three times were measured to determine the hardness.

2.3.10 TGA. TGA experiments were performed on TA-60WS (Shimadzu Co., Ltd, Japan). The hybrid samples were heated from room temperature to 500 °C on an aluminum pan with a heating rate of 10 °C min^{-1} under nitrogen atmosphere (flow rate: 30 mL min^{-1}).

2.3.11 Swelling of NIPU/epoxy hybrid materials in THF. All the hybrid materials were separately put into the THF for 24 h at 25 °C. The swelling degree (SD) was given by the following eqn (3), where m_0 was the initial mass of sample, and m_1 was the mass after swelling in THF for 24 h. After swelling in THF, the sample was dried in a ventilated oven at 80 °C during 24 h. The GC was studied based on eqn (4), where m_2 was the mass of sample after drying process. Based on the weight change analysis of the hybrid materials over time, the cross-linkage can be compared among them.[22]

$$\mathrm{SD} = \frac{m_1 - m_0}{m_0} \times 100\% \quad (3)$$

$$\mathrm{GC} = \frac{m_2}{m_0} \times 100\% \quad (4)$$

3. Result and discussion

3.1 Preparation and analysis of 5CC-PPGDGE

Based on the previous report,[35] further analysis of 5CC-PPGDGE was carried out through FTIR, ^{1}H NMR and elemental analysis.

3.1.1 Characterization of 5CC-PPGDGE. The transformation of epoxy groups to cyclic carbonate groups was confirmed by FTIR as shown in Fig. 1. The spectra provide obvious information about the structure difference between 5CC-PPGDGE and initial PPGDGE. It emphasizes the appearance of new peaks at 1797 cm^{-1} and 1162 cm^{-1} assigned to C=O and C–O of carbonate unit, respectively. The signal peak of epoxy –O– at 907 cm^{-1} doesn't totally disappear, which has been illustrated in our previous report by FTIR with the evolution of time.[35] Here, further analysis was conducted by comparing 5CC-PPGDGE with analogue. Five-membered cyclic carbonate originating from PEGDGE (5CC-PEGDGE), having the similar structure with 5CC-PPGDGE, was chosen (the mechanism and structure is shown in Scheme S1†). The FTIR of 5CC-PEGDGE is adopted to further illustrate the effect of $-CH_3$ in 5CC-PPGDGE. For PEGDGE-based cyclic carbonate, the intensity of epoxy –O– at 907 cm^{-1} disappears after CO_2-fixed reaction. Having analyzed the structure of cyclic carbonate originating from PEGDGE and PPGDGE, the most convincing reason is whether there is $-CH_3$ in repeating unit of molecure structure. Therefore, for 5CC-PPGDGE, the peak intensity at 907 cm^{-1} is attributed to $-CH_3$ partly.

As additional evidence, the formation of cyclic carbonate was further confirmed by ^{1}H NMR (see Fig. 2). From Fig. 2, it is observed that the signal peaks of epoxy group at 2.54 ppm, 2.71 ppm and 3.05 ppm[22] disappear completely in 5CC-PPGDGE. Meanwhile, the new peak signals appeared at 4.29 ppm, 4.51 ppm and 4.90 ppm belong to cyclic carbonate groups. The signal at 4.29 ppm is attributed to the C–H of cyclic carbonate in α-position and signals at 4.51 ppm and 4.90 ppm belong to the hydrogen in β-position of cyclic carbonate group.

It is absolutely clear that the reactants are composed of carbon, hydrogen, and oxygen. The elemental content of PPGDGE and 5CC-PPGDGE is analyzed to provide further information about the insert amount of CO_2 into PPGDGE (see Table 2). The formula calculation is based on PPGDGE having two epoxy groups per molecule. Table 2 reveals that two CO_2 molecules are coupling with PPGDGE which proves that complete conversion of PPGDGE is acquired. And 97.1%

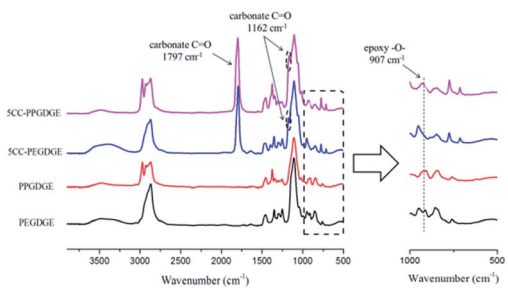

Fig. 1 FTIR spectra of 5CC-PPGDGE compared with analogue.

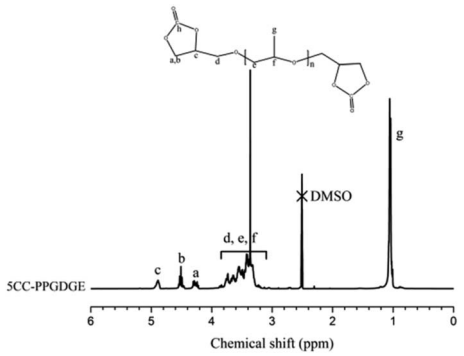

Fig. 2 ^{1}H NMR spectrum of 5CC-PPGDGE.

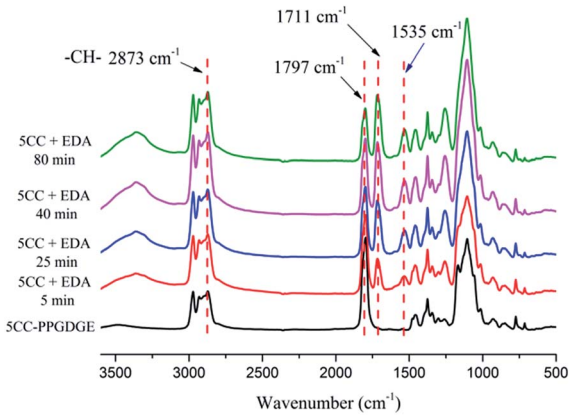

Fig. 3 FTIR of NIPU synthesis from ring-opening reaction of 5CC-PPGDGE and EDA at 25 °C.

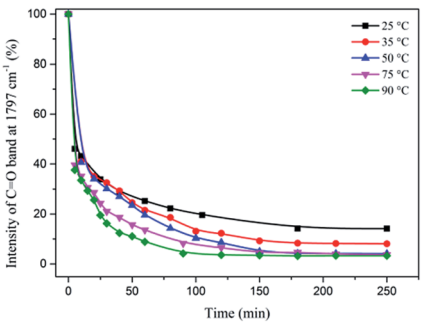

Fig. 4 Kinetics of NIPU synthesis from 5CC-PPGDGE and EDA at different temperature.

selectivity is obtained by elemental analysis, which is in accordance with previous study with a selectivity of 98.8%. Besides, fixed CO_2 amount of about 12 wt% and cyclic carbonate amount of 23 wt% are also achieved from elemental analysis and ^{1}H NMR.

3.1.2 Kinetics of ring-opening reaction of 5CC-PPGDGE with EDA. In order to investigate the reactivity of 5CC-PPGDGE, the ring-opening model reaction of 5CC-PPGDGE with EDA is conducted at different temperature. The progress of 5CC-PPGDGE conversion into NIPU is calculated by the FTIR peak signal of C=O of cyclic carbonate group at 1797 cm^{-1} (see Fig. 3). The reaction temperature was examined at 25 °C, 35 °C, 60 °C, 70 °C and 90 °C. The further increase temperature was not adopted due to the formation of substituted urea through attack of amine molecule.[15]

Fig. 3 shows the FTIR spectra of the process of EDA-based NIPU formation with a stoichiometric ratio at 25 °C. The peak signal of cyclic carbonate groups at 1797 cm^{-1} disappears gradually over time but remains partial cyclic carbonate groups after 80 min due to the low reaction temperature. The formation of EDA-based NIPU or decrease of signal peak at 1797 cm^{-1} as a function of temperature and time is showed in Fig. 4. It is clear that over half of C=O intensity has weakened within 10 min at any reaction temperature. And at 50 °C, 70 °C and 90 °C, almost complete disappear is observed after reaction for at least 180 min. However, the ring-opening reaction conducted at 25 °C and 35 °C is faltering at a conversion of 80% more than 200 min. The main problems of the aminolysis reaction of 5CC-PPGDGE with amine are the long reaction time and low conversion.

It is undeniable that the viscosity increases as the ring-opening reaction proceeds. Effect of viscosity is more prominent at a low temperature due to diffusion of 5CC-PPGDGE. In general, an increase in reaction temperature could be a pretty solution to overcome the high viscosity. Besides, an addition of catalyst could lower the activation energy and accelerate the reaction markedly.

In order to accelerate reaction rate and improve conversion, TEDA is selected as catalyst for the ring-opening reaction. As shown in Fig. 5, the addition of 0.5 wt% TEDA promotes conversion significantly. In the case of only 20% and 10% intensity is achieved within 30 min for reaction at 25 °C and 90 °C, respectively. Subsequently, conversion increases slowly due to high viscosity. And the C=O intensity of carbonate is leveling off at around 10% and 5%. The conversion and rate is further improved than that of reaction in the absence of TEDA. Besides, effect of TEDA on the carbonate conversion is more

Table 2 Properties of PPGDGE and 5CC-PPGDGE

Sample	C[a]	H[a]	O[a]	Formula[a]	Fixed CO_2 (wt%)[b]	Cyclic carbonate (wt%)[b]	Selectivity (%)[b]	Fixed CO_2 (wt%)[c]	Cyclic carbonate (wt%)[c]	CEW (mmol g^{-1})[c]
PPGDGE	58.16	8.81	33.68	$C_{31.81}H_{57.25}O_{13.67}$	—	—	—	—	—	
5CC-PPGDGE	54.32	7.65	38.02	$C_{33.86}H_{57.25}O_{17.77}$	12.06	23.15	97.1	11.73	22.9	2.78

[a] The composition results were determined by elemental analysis. [b] Component of PPGDGE and 5CC-PPGDGE was calculated according to molecular mass and composition. [c] The CO_2 fixed content and CEW were calculated by ^{1}H NMR.[35]

effective at low temperature (25 °C). However, the conversion of 5CC-PPGDGE into NIPU is distinctly different from the five-membered cyclic carbonate propylene oxide (5CC-PO), which has been widely studied.[36] The kinetics of ring-opening reaction of 5CC-PO is shown in Fig. S1.† As illustrated in Fig. S1,† less than 5% carbonate intensity is achieved within 10 min whether or not the TEDA is adopted. The main differences between PPGDGE-based and PO-based carbonate originate from 5CC-PPGDGE with difunctionality and lower reactivity due to high molecular mass (about 750 g mol^{-1}). Meanwhile, with the process of ring-opening reaction, increase of intermolecular force could also lead to low molecular mass of final NIPU product.

Even reaction being conducted at 90 °C with TEDA, the molecular mass (only 5700 g mol^{-1}) is too small to be used as polymer materials, which may be ascribed to the presence of side products, such ureas and oxazolidinones. These side products are responsible for the low molar mass. The initial stoichiometric ratio is destroyed by the side reaction of amine with urethane unites.[25] However, this NIPU with short chain could be as soft segments like polyether in traditional polyurethane materials. Therefore, in following study, the 5CC-PPGDGE-based NIPU with short chain would be acted as pre-polymer and soft segment for final materials.

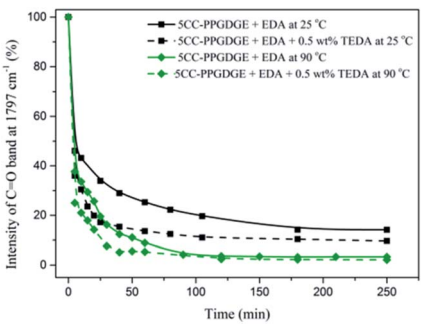

Fig. 5 NIPU synthesis with TEDA compare with NIPU formation with no catalyst.

3.2 Preparation of NIPU pre-polymers

Series of NIPU pre-polymers with NH_2-terminated structure and different molecular mass were formed. The excessive amine is essential to form NH_2-terminated structure and raise 5CC-PPGDGE conversion. The relationship between structure and amine content is further studied than our previous research by adjusting EDA, DETA and TETA molar ratio, compared to 5CC-PPGDGE. The soft segment NIPU pre-polymer has great influence on the performances of final materials. Therefore, pre-polymers were investigated by ^{1}H NMR, FTIR, and GPC (formulations of pre-polymers have been shown in Table 3).

3.2.1 The structure characterization of NIPU pre-polymers. All NIPU pre-polymers were prepared according to Scheme 2. Pre-polymer-EDA-1 and Pre-polymer-EDA-4 had been selected as model compounds to illustrate the formation of NH_2-terminated structure of pre-polymer by ^{1}H NMR (see Fig. 6). The signals of cyclic carbonate at 4.29–4.90 ppm disappear completely for Pre-polymer-EDA-4, but remain 10% for pre-polymer-EDA-1, accurately calculated according to eqn (2). Meanwhile, for both pre-polymers, new peak signals at 3.63–3.74 ppm and 3.03 ppm correspond to $-CH_2-$ in α and β position of $-NH_2$, respectively, which proves the functionalization of pre-polymer by primary amine groups terminated. Besides, the ^{1}H NMR spectra also show the signal assigned to excessive EDA at 2.61 ppm.

The FTIR spectra of these pre-polymers are shown in Fig. 7 and Fig. S2.† The peak signals at 1711 cm^{-1}, 1535 cm^{-1} and 1256 cm^{-1} are assigned to urethane groups. However, for all pre-polymers with lowest amine ratio, spectra display a small peak of peak of carbonate moieties, which might be caused by the mass transfer resistance encountered at high viscosity. In addition, the ring-opening reaction of 5CC-PPGDGE with excessive amine hasn't resulted in the formation of amide

Table 3 The molecular weight and viscosity of per-polymers at various amine ratios

Sample	Type of amine	Amine: (5CC-PPGDGE + BADGE)[a]	Amine: 5CC-PPGDGE[b]	Mn (g mol^{-1})[c]	Viscosity at 70 °C (Pa s)
Pre-polymer-EDA-1	EDA	0.7	1.14	4000	2.68
Pre-polymer-EDA-2	EDA	0.9	1.46	3200	2.04
Pre-polymer-EDA-3	EDA	1.1	1.79	2500	1.58
Pre-polymer-EDA-4	EDA	1.3	2.11	2250	1.41
Pre-polymer-DETA-1	DETA	0.7	1.05	2600	2.36
Pre-polymer-DETA-2	DETA	0.9	1.35	1900	2.02
Pre-polymer-DETA-3	DETA	1.1	1.65	1600	1.51
Pre-polymer-DETA-4	DETA	1.3	1.96	1400	1.32
Pre-polymer-TETA-1	TETA	0.7	1.01	2400	1.75
Pre-polymer-TETA-2	TETA	0.9	1.28	1800	1.53
Pre-polymer-TETA-3	TETA	1.1	1.56	1400	1.40
Pre-polymer-TETA-4	TETA	1.3	1.85	1300	1.34

[a] The amine ratio varied by altering the proportion to 5CC-PPGDGE and BADGE, and the corresponding BADGE content in final materials was fixed to 40 wt%. [b] Compared to 5CC-PPGDGE, the relative content of amine was determined. [c] Mn of pre-polymers were analyzed by GPC and calculated from the starting materials. The test samples were treated by distilling under vacuum.

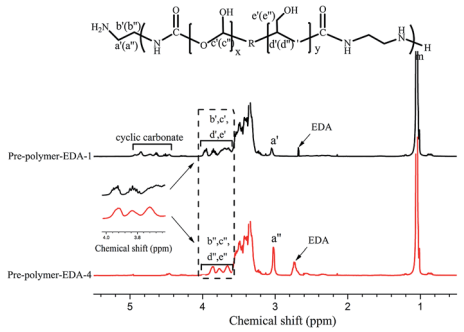

Fig. 6 ^{1}H NMR spectra for both Pre-polymer-EDA-1 and Pre-polymer-EDA-4.

groups, which is of great difference with that of soybean oil-based cyclic carbonate.[37]

3.2.2 The GPC of NIPU pre-polymers. The apparent number-average molecular mass (M_n) of these pre-polymers is shown in Table 3. The M_n values vary with altered the amine ratio and amine type. The molecular mass of NIPU from ring-opening reaction between cyclic carbonate and amine has been reported by many groups,[38–40] and low M_n value is not completely resolved. One possible reason should be side reactions due to the high reaction temperature and mole ratio of the reactants.[37] In this study, the general by-products, such as amide and urea, are not detected by FTIR and ^{1}H NMR, which indicate the side reaction during this ring-opening reaction between 5CC-PPGDGE and amine could be negligible.

From Table 3, M_n values are affected by amine ratio and type. The increase of amine ratio is conducive to the aminolysis of cyclic carbonate and the termination of pre-polymer with primary amine, which restrict the growth of M_n. Meanwhile, the secondary amine in DETA and TETA might react with cyclocarbonate partially, which restricts the movement and reduces the reactivity of segment chain. Consequently, the pre-polymers obtained from TETA and DETA have lower M_n values than that of EDA-based ones.

3.3 Synthesis and characterizations of NIPU/epoxy hybrid polymers

The NH_2-terminated soft NIPU pre-polymers were cured by introducing BADGE as chain extender to prepare NIPU/epoxy hybrid materials (Scheme 3). The BADGE was adopted to accelerate the cure rate, increase cross-linkage and improve performance of materials. It was found that reactants ratio had great effect on the properties of final NIPU/epoxy hybrid materials. In this study, further research has been done to study the effect of amine type and ratio on the controlled architectures of final materials when the BADGE content was fixed to 40 wt%.

The appearance of these NIPU/epoxy hybrid materials was shown in Fig. 8. For all formulations of these materials, all samples were presented light yellow and transparent solid samples in appearance.

3.3.1 FTIR. Fig. 9 and S3† show the FTIR spectra of all NIPU/epoxy hybrid materials. For all the spectra, there are stronger vibration peaks of O–H and N–H stretching appeared at 3100–3500 cm^{-1} than that of corresponding pre-polymers, which proves the reaction between amine groups and epoxy of BADGE. The peaks at 1605 cm^{-1}, 1581 cm^{-1} and 1511 cm^{-1} are assigned to C=C vibration of benzene skeleton of BADGE which illustrates the BADGE is introduced to pre-polymer successfully. The ranges at 1250–1000 cm^{-1} are in-plane bending vibration of C–H of benzene structure. In addition, peaks at 1711 cm^{-1} and 1535 cm^{-1} belong to the C=O and N–H of urethane groups. However, for spectrum of NIPU-EDA-1 with the lowest amine content, the absorption peak at 1797 cm^{-1} confirms residual cyclic carbonate in final product, which reflects the incomplete cross-linked network for the material. This residual peak doesn't exist in spectra of NIPU-DETA-1 and NIPU-TETA-1 (shown in Fig. S3†). It could be interpreted that DETA and TETA provide higher reactivity or more reactive sites than EDA, which leads to further reaction of residual cyclic carbonate groups with amine during the curing process.

3.3.2 SEM. Fig. 10 presents the morphologies of fractured surfaces of NIPU-EDA-1, NIPU-EDA-3, NIPU-DETA-3 and NIPU-TETA-3. These are small particles dispersed in the matrix of NIPU-EDA-1 on the fractured surface. It reveals that the poor microstructures are formed in NIPU-EDA-1, which is consistent with the FTIR results. However, with the increase of amine ratio and functionality, there are no manifest dispersed particles in the surfaces due to the formation of perfect structure. In addition, the NIPU-TETA-3 obtains the continuous morphology, which indicates the more functionality of TETA improves cross-link density of the hybrid materials.

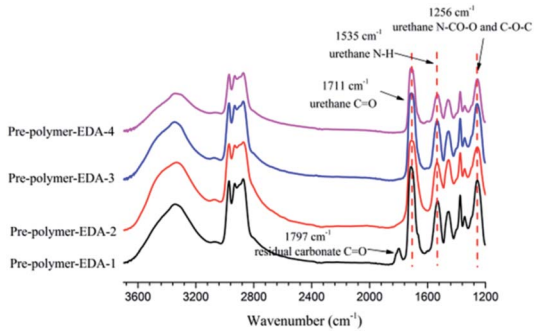

Fig. 7 FTIR spectra of pre-polymers preparing from EDA.

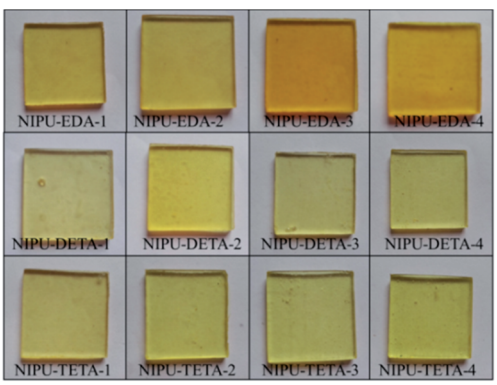

Fig. 8 The appearance of final NIPU/epoxy hybrid materials.

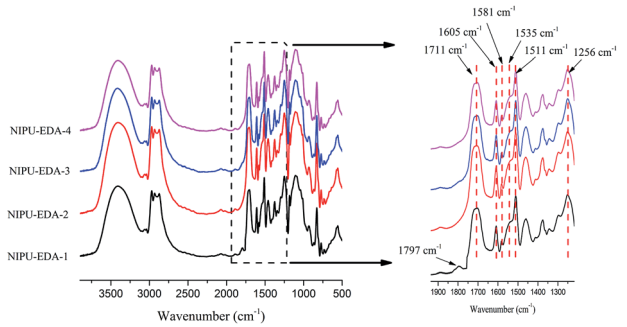

Fig. 9 FTIR spectra for EDA-based NIPU/epoxy hybrid materials.

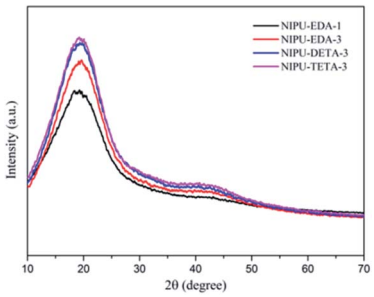

Fig. 11 XRD of selected hybrid materials.

3.3.3 XRD. The structure of the selected hybrid materials are also determined by XRD analysis in Fig. 11. A broad diffraction peak from 10° to 28° is caused by scattering of the hybrid materials molecules, which might be ascribed to the amorphous nature or presence of small amounts of crystalline structure. BADGE reacts with the NH_2-terminated pre-polymer to form cross-linked network, which results in reducing the flexibility of segments and limiting overall backbone mobility. Besides, the increase of diffraction peak intensity of NIPU-TETA-3 is produced indicating an increase in crystallinity, which proves the NIPU-TETA-3 obtains better structure.

3.3.4 The cross-linkage analysis of NIPU/epoxy hybrid materials by swelling in THF. Swelling in solvents gives additional information on the structure of NIPU/epoxy hybrid materials. SD and GC of these products were performed by swelling in THF to evaluate the cross-linkage density. Table 4 and Fig. 12 summarized all values of SD and GC obtained for all the formulations. The results illustrates swelling in THF strongly depends on amine ratio as well as the amine type. SD values of EDA-based, DETA-based and TETA-based hybrid materials climb up with amine ratio increasing. It is caused by the solubility of polymer in solvent due to primary or secondary amine groups and hydroxyl polarizing the polymer material. Meanwhile, the presence of polar groups makes these materials susceptible to solvent.[37] NIPU-EDA-4 with the highest EDA ratio, for example, obtains the highest SD value of about 135%, yet the SD of EDA-NIPU-1 is only 93.3% caused by the lowest amine content and low hydroxyl groups. The same trend is observed among DETA-based and TETA-based ones. In addition, the TETA-based hybrid materials have the lowest SD values among these hybrid materials due to perfect cross-linked network structure.

As for GC of NIPU/epoxy hybrid materials from EDA, it is ranged between 85% and 94.4% which proves the high cross-linkage networks only contain less than 15% of soluble chains. Additionally, DETA-based and TETA-based hybrid materials display the higher GC with variation range of 94.1% to 96.2% and 95.3% to 97.4%, respectively, which is a result of denser network than that of EDA-based ones. Interestingly, for hybrid materials of these three types, GC increases first and then declines with the increase of amine ratio. The trend is controlled by cross-linkage architectures and linear degree of hybrid materials (as is shown in Scheme 3). The least amine ratio gives poor conversion of carbonate or epoxy to urethane and hydroxyls, which limits the formation of chemical and physical cross-linkage, even causing the existence of soluble chain.[41] Along with the amine ratio increase, the cross-linkage architectures are improved and tend to be more ideal (see Scheme 3(I) and (II)). Also, GC of hybrid materials with the highest amine ratio is slightly lower than the 1.1 amine ratio ones, which proves the structural integrity. The structure of these hybrid materials is close to linear structure (Scheme 3(III)). Therefore, the structure of these hybrid materials could be controlled well by adjusting the amine ratio and type. The various architectures have great and different effects on properties of NIPU/epoxy hybrid materials.

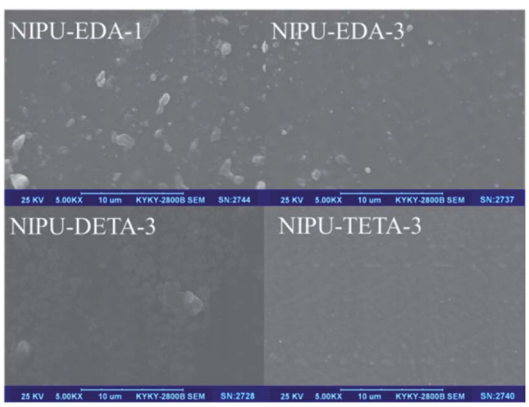

Fig. 10 SEM of selected hybrid materials.

3.3.5 Mechanical performance. The tensile properties and hardness of all formulations are summarized in Table 4. Stress–strain curves of these hybrid materials are plotted in Fig. 13 and S4.† These NIPU/epoxy hybrid materials display satisfactory mechanical performance. For example, hybrid materials derived from DETA could obtain various tensile strength from 7.3 MPa to 16.0 MPa accompanied by elongation at a range of 71.8% to 151.3%. Especially, NIPU-DETA-4 obtains excellent tensile strength of 15 MPa with elongation at break over 150%. Surprisingly, TETA-based hybrid material with amine ratio at 1.3, NIPU-TETA-4, has elongation at break over 170.9% accompanied by tensile strength of 12.5 MPa. The hybrid materials in this report are demonstrated better comprehensive mechanical properties than many NIPU prepared from the similar method. For example, Stroganov and co-workers

Table 4 Composition, swelling properties in THF, tensile performance and hardness test of NIPU/epoxy hybrid materials

Sample[a]	SD[b] (%)	GC[b] (%)	Tensile strength[c] (MPa)	Elongation at break[c] (%)	Young's modulus[c] (MPa)	Hardness (shore A)[c]
NIPU-EDA-1	93.3	85.0	4.0 ± 0.2	156.5 ± 12.3	1.7 ± 0.4	80
NIPU-EDA-2	101.5	94.9	13.6 ± 0.6	105.7 ± 15.6	60.4 ± 8.8	84
NIPU-EDA-3	113.6	94.4	14.8 ± 0.4	79.9 ± 6.5	128.4 ± 8.7	87
NIPU-EDA-4	135.8	93.2	12.2 ± 0.6	152.3 ± 7.4	99.0 ± 7.6	85
NIPU-DETA-1	87.6	94.6	7.3 ± 1.1	141.2 ± 12.9	16.8 ± 5.2	88
NIPU-DETA-2	87.2	96.2	14.8 ± 0.6	71.8 ± 11.6	89.6 ± 7.4	92
NIPU-DETA-3	98.3	95.3	16.0 ± 0.8	98.3 ± 8.6	124.1 ± 5.5	91
NIPU-DETA-4	109.1	94.1	15.0 ± 1.6	151.3 ± 18.9	99.9 ± 3.3	89
NIPU-TETA-1	73.6	95.3	10.4 ± 2.1	94.0 ± 14.3	42.9 ± 12.7	92
NIPU-TETA-2	82.5	97.0	13.6 ± 1.3	89.0 ± 34.8	89.3 ± 8.7	94
NIPU-TETA-3	93.9	97.4	15.8 ± 0.4	122.4 ± 19.4	125.6 ± 8.4	91
NIPU-TETA-4	105.5	96.8	12.5 ± 0.9	138.4 ± 6.4	38.4 ± 6.4	90

[a] The content of BADGE in final hybrid materials was 40 wt%. [b] Swelling degree (SD) and gel content (GC) were measured by swelling in THF. [c] Values were reported as average of three specimens.

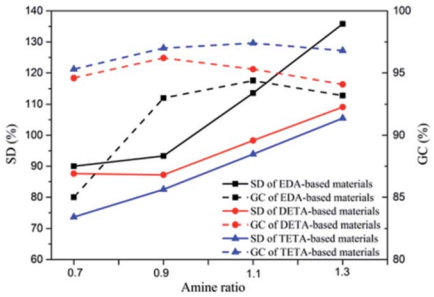

Fig. 12 SD and GC of NIPU/epoxy hybrid materials.

obtained the NIPU/epoxy materials with tensile strength above 18 MPa but maximum elongation at break of only 5.2%.[42] Cornille *et al.* prepared the NIPU/epoxy hybrid materials from different epoxy resin with poor mechanical properties.[43] Besides, Leitsch *et al.* obtained the similar polyurethane/NIPU hybrid polymers which had the tensile strength at 4.5 MPa but strain at 350%.[44] It could be found that our hybrid materials exhibit a good balance among the tensile strength and elongation at break. Especially, the mechanical properties are controlled by altering amine type and ratio.

For these three type hybrid materials, increase of amine ratio leads to the tensile strength, Young's modulus and hardness following the trend of increasing first and then decreasing. But

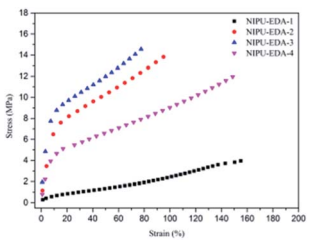

Fig. 13 Representative stress–strain curves of EDA-based hybrid materials.

the opposite result is occurred in elongation at break. Meanwhile, increase of functional groups of amine leads to increase in Young's modulus, tensile strength and hardness as a direct consequence of the improvement of cross-linked structure.

Further analysis of these results, for EDA-based materials as example, NIPU-EDA-1 displays elongation at break over 150%, and it decreases to about 80% when the amine ratio was added to 1.1. However, the elongation increases over 150% again as a result of the amine ratio at 1.3. This could be interpreted that (i) when amine ratio is low, network structure is insufficiently cured as observed from the FTIR and GC analysis, resulting in low cross-linkage and residual cyclic carbonate groups which has a plasticizing function for hybrid material.[45] (ii) With the amine ratio increased, the cross-linked structure is improved, which leads to elongation at break shortening while tensile strength and Young's modulus increasing. (iii) With further more amine ratio, the configuration of material tends to be more linear structure. It is clear that the NIPU-EDA-4 with the highest amine ratio has much higher elongation but the tensile strength is only slightly decreased. This proves the structural integrity of NIPU-EDA-4 as the results of GC. Similar results could be observed in DETA-based and TETA-based hybrid materials. On the other hand, DETA-based and TETA-based materials have similar elongation and higher tensile strength than that of EDA-based ones. It might be caused by the difference in reactivity of primary and secondary amine groups. The terminal primary amine of pre-polymer reacts with epoxy firstly, meanwhile, causing a reduced accessibility of secondary amine. And the secondary amine groups could act as plasticizers for the hybrid material.[46] Therefore, the DETA-based and TETA-based materials have both high tensile strength and well elongation at break.

3.3.6 DMA. DMA results of prepared hybrid materials are shown in Table 5 and Fig. 14a–c. The presence of one peak of tan δ curves in Fig. 14 is exhibited and the corresponding temperature is usually acted as mechanical transition temperature, also called T_g, which is related to initial motion of chain

segments of molecular chains. Table 5 lists the T_g values for all materials. The T_g values vary in the range of 36 to 44 °C for EDA-based hybrid materials, 38 to 43 °C for DETA-based hybrid materials, and 43 to 47 °C for TETA-based ones. The higher T_g in TETA-based samples could be attributed to the more functional groups of TETA in comparison to EDA and DETA. However, there are much difference on T_g of NIPU/epoxy which are prepared from the same method. For example, the T_g of NIPU/epoxy hybrid materials from literatures[42,46] are much higher than our work, which is attributed to the higher hard segment content from the epoxy resin. However, compared to our work, the hybrid NIPU/epoxy materials reported from Cornille *etc.*[43] have lower T_g, which is the result of the poor cross-linking. Hence, the T_g is much determined by the composition and structure of these NIPU/epoxy hybrid materials.

It is clear from the T_g values of hybrid materials, with the increase of amine ratio, the trend of change of T_g values is the same as GC, tensile strength and hardness. Residual cyclic carbonate groups and imperfect structure cause the low T_g value for the materials. In pace with increasing amine ratio, the T_g value increases due to further reaction of cyclic carbonate and formation of denser crosslinking network. It is attributed to the limited motion of segments in materials.[47] However, with further increase of amine ratio, the T_g value decreases owing to loss of cross-linkage and formation of linear structure.

It is fascinating that the peak height of tan δ curves goes up with increasing amine ratio, which illustrates increase of the ability of energy dissipation. However, the extraordinary result is found that the change trend of T_g values, for EDA-based hybrid materials as example, was inconsistent with that of peak height of tan δ, which is contrary to previous reports.[45] It might be the result different architectures caused by the amine ratio (unreacted cyclic carbonate groups remained in system, and the molecular chain structure was cross-linkage or linear).

Table 5 and Fig. 14a–c also shows the values of tan δ over a different temperature range. These temperature ranges could represent some special structural application. Among the three materials, the EDA-based materials have the values of tan $\delta \geq$ 0.3 over a temperature range of $\geq$ 90 °C. However, the values of

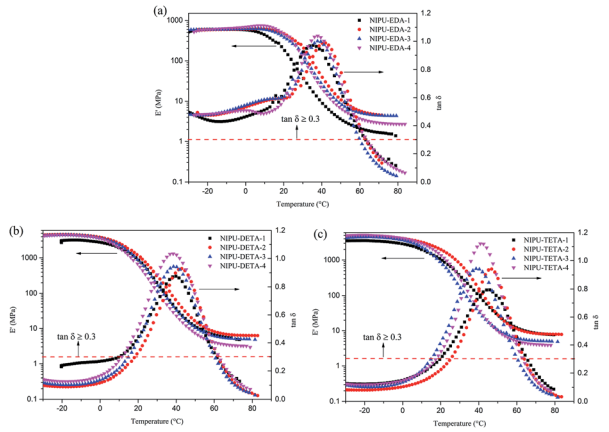

Fig. 14 Temperature dependences of storage modulus (E') and tan δ obtained from DMA. (a) EDA-based hybrid materials, (b) DETA-based hybrid materials, (c) TETA-based hybrid materials.

DETA-based and TETA-based materials were manifested in sharp tan δ peaks (tan $\delta \geq 0.3$) over a narrower range of temperature at 44–53 °C and 39–46 °C, respectively. tan $\delta \geq 0.3$ is used as criterion for damping properties of materials, which reveals that these hybrid materials from EDA might serve as sound and vibration damping materials.[19]

3.3.7 TGA. The thermodynamic stability of these NIPU/epoxy hybrid materials were evaluated with TGA analysis in the range of ambient temperature to 500 °C (Fig. 15a, b, S5 and S6†). Table 5 shows the T_{onset}, T_d(5%), T_d(50%) and char at 500 °C of all the hybrid materials. It is clear from the Table 5 that DETA-based and TETA-based hybrid materials have the more excellent T_{onset} than EDA-based ones, which is the result of the dense cross-linking network due to the polyfunctional groups of DETA and TETA. Meanwhile, for the NIPU/epoxy hybrid materials prepared from the same type of amine, the materials with perfect architectures have higher T_{onset} and char, such as NIPU-EDA-3, NIPU-DETA-3 and NIPU-TETA-3. However, the materials having linear structure and poor cross-linkage obtain lower T_{onset} and char.

Table 5 DMA and TGA test of NIPU/epoxy hybrid materials

Sample	T_g (°C)/tan δ peak[a]	T (tan $\delta \geq 0.30$) (°C)[b]	ΔT (°C)[b]	T_{onset} (°C)[c]	T_d (5%) (°C)[c]	T_d (50%) (°C)[c]	Char at 500 °C(%)[c]
NIPU-EDA-1	36	~30 to 63	>93	236	263	358	12
NIPU-EDA-2	44	~30 to 67	>97	250	288	359	16
NIPU-EDA-3	39	~30 to 65	>95	257	280	364	17
NIPU-EDA-4	38	~30 to 63	>93	248	268	369	14
NIPU-DETA-1	39	18 to 62	44	251	274	361	10
NIPU-DETA-2	43	18 to 62	44	252	276	366	14
NIPU-DETA-3	39	15 to 60	45	259	274	370	17
NIPU-DETA-4	38	11 to 63	53	249	271	364	11
NIPU-TETA-1	45	20 to 66	46	248	274	366	8
NIPU-TETA-2	47	25 to 44	39	258	282	371	11
NIPU-TETA-3	44	20 to 64	44	258	280	371	17
NIPU-TETA-4	43	16 to 62	46	253	280	369	10

[a] The temperature of tan δ peak is defined as T_g. [b] The temperature range of value of tan δ is over 0.3. [c] The temperature of mass loss 5% and 50% and chat at 500 °C is determined by TGA. The T_{onset} is initial degradation temperature of sample.

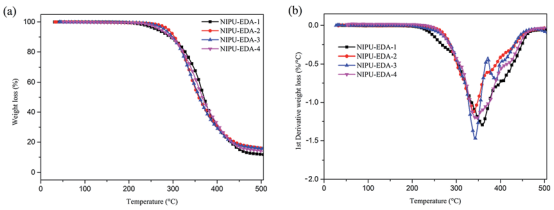

Fig. 15 TGA (a) and DTGA (b) curves of EDA-based hybrid materials under nitrogen.

Besides, as Fig. 15b shows, these samples exhibit good thermodynamic stability until about 220 °C. The degradation temperature of 5% mass loss of all samples is over 260 °C, which is the typical degradation temperature of urethane linkages. And at 50% weight loss, the corresponding degradation temperature exhibits a distinct difference. For hybrid materials with 1.1 amine ratio, the highest temperature is obtained at 364 °C, 370 °C and 371 °C for NIPU-EDA-3, NIPU-DETA-3 and NIPU-TETA-3, respectively, which indicates that the formation of high thermodynamic stable network. But for the others, the lowest degradation at 50% weight loss is observed for the samples with the lowest amine ratio, which is caused by the poor cross-linkage network. Due to the denser cross-linkage network provided by TETA, TETA-based materials possess the highest thermodynamic stability, following by the DETA-based and EDA-based ones.

4. Conclusions

In this work, polyurethane/epoxy hybrid materials were prepared *via* an environment-friendly and non-toxic route, which avoided the use of toxic isocyanate. Meanwhile, PPGDGE was selected to fix CO_2 with a complete conversion. The selectivity of 97.1% of this CO_2-sourced monomer was acquired through elemental analysis. CO_2 fixation content was determined by elemental analysis at 12.06 wt% and ^{1}H NMR at 11.73 wt%. The kinetics of 5CC-PPGDGE was also investigated by reacting cyclic carbonate with EDA at different temperature. And TEDA was determined as catalyst for the reaction of 5CC-PPGDGE with amine. Three series of NH_2-terminated NIPU pre-polymers were successfully prepared and the importance of amine ratio and functionality was highlighted. For the final NIPU/epoxy hybrid materials cured by BADGE, the architectures and properties were controlled by varying amine ratio and type. This was the first time to control the architectures of these hybrid materials by altering amine ratio and functionality. The structure of hybrid materials were analysed by FTIR, SEM, XRD and swelling in THF, which indicated that hybrid materials with low amine ratio had imperfect cross-linked network and it had been improved gradually with the increased amine ratio increase. Meanwhile, hybrid materials prepared from polyfunctionality amine had more excellent mechanical and thermal properties. Especially, NIPU-DETA-4 and NIPU-TETA-4 exhibited high tensile strength of 15.0 MPa and 12.5 MPa, accompanied with elongation at break at 151.3% and 170.9%, respectively. However, EDA-based hybrid materials had better energy dissipation ability than DETA-based and TETA-based ones, which can be potential barrier material.

Acknowledgements

The authors gratefully thank the financial support from "the Major Science & Technology Project of Shanxi Provence (No. MD2014-10)" and "Youth scientific funds of Shanxi Provence (No. 2015021043)".

References

1 B. F. Cai, J. N. Wang, J. He and Y. Geng, *Appl. Energy*, 2016, **166**, 191–200.
2 C. H. Huang and C. S. Tan, *Aerosol Air Qual. Res.*, 2014, **14**, 480–499.
3 N. Yang and R. Wang, *J. Cleaner Prod.*, 2015, **103**, 784–792.
4 L. Li, N. Zhao, W. Wei and Y. H. Sun, *Fuel*, 2013, **108**, 112–130.
5 W. Dai, S. Luo, S. Yin and C. Au, *Front. Chem. Sci. Eng.*, 2010, **4**, 163–171.
6 Z. Z. Yang, Y. N. Zhao and L. N. He, *RSC Adv.*, 2011, **1**, 545–567.
7 Q. Chen, C. Peng, H. Xie, Z. k. Zhao and M. Bao, *RSC Adv.*, 2015, **5**, 44598–44603.
8 J. O. Akindoyo, M. D. H. Beg, S. Ghazali, M. R. Islam, N. Jeyaratnam and A. R. Yuvaraj, *RSC Adv.*, 2016, **6**, 114453–114482.
9 S. H. Choi, D. H. Kim, A. V. Raghu, K. R. Reddy, H. I. Lee, K. S. Yoon, H. M. Jeong and B. K. Kim, *J. Macromol. Sci., Part B: Phys.*, 2012, **51**, 197–207.
10 K. R. Reddy, A. V. Raghu and H. M. Jeong, *Polym. Bull.*, 2008, **60**, 609–616.
11 R. W. Carolyn, N. J. Anderson and D. K. Bonauto, *J. Occup. Environ. Hyg.*, 2013, **10**, 597–608.
12 R. J. Slocombe, E. E. Hardy, J. H. Saunders and R. L. Jenkins, *J. Am. Chem. Soc.*, 1950, **72**, 1888–1891.
13 H. Blattmann, M. Fleischer, M. Bahr and R. Mulhaupt, *Macromol. Rapid Commun.*, 2014, **35**, 1238–1254.
14 J. M. Raquez, M. Deleglise, M. F. Lacrampe and P. Krawczak, *Prog. Polym. Sci.*, 2010, **35**, 487–509.
15 A. Cornille, R. Auvergne, O. Figovsky, B. Boutevin and S. Caillol, *Eur. Polym. J.*, 2016, **87**, 535–552.
16 L. Maisonneuve, O. Lamarzelle, E. Rix, E. Grau and H. Cramail, *Chem. Rev.*, 2015, **115**, 12407–12439.
17 P. Krol, *Prog. Mater Sci.*, 2007, **52**, 915–1015.
18 M. S. Kathalewar, P. B. Joshi, A. S. Sabnis and V. C. Malshe, *RSC Adv.*, 2013, **3**, 4110.
19 E. K. Leitsch, G. Beniah, K. Liu, T. Lan, W. H. Heath, K. A. Scheidt and J. M. Torkelson, *ACS Macro Lett.*, 2016, **5**, 424–429.
20 K. R. Reddy, A. V. Raghu, H. M. Jeong and Siddaramaiah, *Des. Monomers Polym.*, 2009, **12**, 109–118.
21 A. Cornille, C. Guillet, S. Benyahya, C. Negrell, B. Boutevin and S. Caillol, *Eur. Polym. J.*, 2016, **84**, 873–888.
22 A. Cornille, G. Michaud, F. Simon, S. Fouquay, R. Auvergne, B. Boutevin and S. Caillol, *Eur. Polym. J.*, 2016, **84**, 404–420.

23 R.-j. Wei, X.-h. Zhang, B.-y. Du, Z.-q. Fan and G.-r. Qi, *RSC Adv.*, 2013, **3**, 17307.
24 M. Bähr, A. Bitto and R. Mülhaupt, *Green Chem.*, 2012, **14**, 1447.
25 M. Bähr and R. Mülhaupt, *Green Chem.*, 2012, **14**, 483.
26 S. Wang, Y. Li and H. Liu, *Acta Chim. Sin.*, 2012, **70**, 1897.
27 W. Shuai and H. Liu, *Catal. Lett.*, 2007, **117**, 62–67.
28 L. Liu and X. P. Ye, *Fuel Process. Technol.*, 2015, **137**, 55–65.
29 V. Besse, F. Camara, F. Mechin, E. Fleury, S. Caillol, J. P. Pascault and B. Boutevin, *Eur. Polym. J.*, 2015, **71**, 1–11.
30 R. M. Garipov, V. A. Sysoev, V. V. Mikheev, A. I. Zagidullin, R. Y. Deberdeev, V. I. Irzhak and A. A. Berlin, *Dokl. Phys. Chem.*, 2003, **393**, 289–292.
31 O. L. Figovsky, L. Shapovalov and O. Axenov, *Surf. Coat. Int., Part B*, 2004, **87**, 83–90.
32 H. Blattmann and R. Mülhaupt, *Green Chem.*, 2016, **18**, 2406–2415.
33 M. Fleischer, H. Blattmann and R. Mülhaupt, *Green Chem.*, 2013, **15**, 934.
34 B. Grignard, J. M. Thomassin, S. Gennen, L. Poussard, L. Bonnaud, J. M. Raquez, P. Dubois, M. P. Tran, C. B. Park, C. Jerome and C. Detrembleur, *Green Chem.*, 2016, **18**, 2206–2215.
35 J. Ke, X. Li, F. Wang, M. Kang, Y. Feng, Y. Zhao and J. Wang, *J. CO2 Util.*, 2016, **16**, 474–485.
36 Y. Du, F. Cai, D.-L. Kong and L.-N. He, *Green Chem.*, 2005, **7**, 518.
37 I. Javni, D. P. Hong and Z. S. Petrović, *J. Appl. Polym. Sci.*, 2008, **108**, 3867–3875.
38 G. Beniah, K. Liu, W. H. Heath, M. D. Miller, K. A. Scheidt and J. M. Torkelson, *Eur. Polym. J.*, 2016, **84**, 770–783.
39 H. Tomita, F. Sanda and T. Endo, *J. Polym. Sci., Polym. Chem.*, 2001, **39**, 860–867.
40 H. Tomita, F. Sanda and T. Endo, *J. Polym. Sci., Polym. Chem.*, 2001, **39**, 851–859.
41 I. Javni, D. P. Hong and Z. S. Petrović, *J. Appl. Polym. Sci.*, 2013, **128**, 566–571.
42 I. V. Stroganov and V. F. Stroganov, *Polym. Sci., Ser. C*, 2007, **49**, 258–263.
43 A. Cornille, J. Serres, G. Michaud, F. Simon, S. Fouquay, B. Boutevin and S. Caillol, *Eur. Polym. J.*, 2016, **75**, 175–189.
44 E. K. Leitsch, W. H. Heath and J. M. Torkelson, *Int. J. Adhes. Adhes.*, 2016, **64**, 1–8.
45 R. Ghanbaralizadeh, H. Bouhendi, K. Kabiri and M. Vafayan, *J. CO2 Util.*, 2016, **16**, 225–235.
46 P. G. Parzuchowski, M. Jurczyk-Kowalska, J. Ryszkowska and G. Rokicki, *J. Appl. Polym. Sci.*, 2006, **102**, 2904–2914.
47 Y. He, D. Xie and X. Zhang, *J. Mater. Sci.*, 2014, **49**, 7339–7352.

